Organization and Evolution of Brain Lipidome Revealed by Large-Scale Analysis of Human, Chimpanzee, Macaque, and Mouse Tissues

ARTICLE *in* NEURON · FEBRUARY 2015

Impact Factor: 15.05 · DOI: 10.1016/j.neuron.2015.01.003 · Source: PubMed

Report

Neuron

Organization and Evolution of Brain Lipidome Revealed by Large-Scale Analysis of Human, Chimpanzee, Macaque, and Mouse Tissues

Highlights

- Brain lipid composition is distinct from that of non-neural tissues
- The lipidome complexity of the brain increases from mice to humans
- Lipid concentrations evolved four times faster in brain than in non-neural tissues
- Evolution of brain lipid concentrations is further accelerated in the human neocortex

Authors

Katarzyna Bozek, Yuning Wei, ..., Patrick Giavalisco, Philipp Khaitovich

Correspondence

giavalisco@mpimp-golm.mpg.de (P.G.), khaitovich@eva.mpg.de (P.K.)

In Brief

Lipids compose the bulk of the nervous system. Bozek et al. uncover the strikingly rapid evolution of lipids in the primate brain and, even more so, in the human neocortex. The authors propose that lipids contributed to the unique capacities of our brains.

Bozek et al., 2015, Neuron *85*, 695–702
February 18, 2015
http://dx.doi.org/10.1016/j.neuron.2015.01.003

CellPress

Neuron
Report

Organization and Evolution of Brain Lipidome Revealed by Large-Scale Analysis of Human, Chimpanzee, Macaque, and Mouse Tissues

Katarzyna Bozek,[1,2] Yuning Wei,[1] Zheng Yan,[1] Xiling Liu,[1] Jieyi Xiong,[1] Masahiro Sugimoto,[3] Masaru Tomita,[3] Svante Pääbo,[2] Chet C. Sherwood,[4] Patrick R. Hof,[5] John J. Ely,[6] Yan Li,[7] Dirk Steinhauser,[7] Lothar Willmitzer,[7] Patrick Giavalisco,[7,*] and Philipp Khaitovich[1,2,8,*]

[1]CAS Key Laboratory of Computational Biology, CAS-MPG Partner Institute for Computational Biology, 320 Yue Yang Road, Shanghai 200031, China
[2]Max Planck Institute for Evolutionary Anthropology, Deutscher Platz 6, 04103 Leipzig, Germany
[3]Institute for Advanced Biosciences, Keio University, 997-0035 Tsuruoka, Yamagata, Japan
[4]Department of Anthropology, The George Washington University, Washington, DC 20052, USA
[5]Fishberg Department of Neuroscience and Friedman Brain Institute, Icahn School of Medicine at Mount Sinai, New York, NY 10029, USA
[6]Alamogordo Primate Facility, Holloman AFB, Alamogordo, NM 88330, USA
[7]Max Planck Institute for Molecular Plant Physiology, Am Mühlenberg 1, 14476 Potsdam, Germany
[8]Skoltech Center for Computational and Systems Biology, Skolkovo Institute for Science and Technology, Skolkovo 143025, Russia
*Correspondence: giavalisco@mpimp-golm.mpg.de (P.G.), khaitovich@eva.mpg.de (P.K.)
http://dx.doi.org/10.1016/j.neuron.2015.01.003

SUMMARY

Lipids are prominent components of the nervous system. Here we performed a large-scale mass spectrometry-based analysis of the lipid composition of three brain regions as well as kidney and skeletal muscle of humans, chimpanzees, rhesus macaques, and mice. The human brain shows the most distinct lipid composition: 76% of 5,713 lipid compounds examined in our study are either enriched or depleted in the human brain. Concentration levels of lipids enriched in the brain evolve approximately four times faster among primates compared with lipids characteristic of non-neural tissues and show further acceleration of change in human neocortical regions but not in the cerebellum. Human-specific concentration changes are supported by human-specific expression changes for corresponding enzymes. These results provide the first insights into the role of lipids in human brain evolution.

INTRODUCTION

Lipids represent an essential structural and functional component of tissues and cells. Initially considered only as the building material of membranes or as a bioenergetic fuel, lipids are now also regarded as signaling messengers in neural tissues and the brain, where they make up half of the organ's dry weight (Piomelli et al., 2007). By regulating the chemical and mechanical properties of membranes, lipids influence vesicle fusion and fission processes, ion flux, and lateral diffusion of membrane proteins (Jacobson et al., 2007; Rohrbough and Broadie, 2005). The distinct architecture of lipids therefore creates microenvironments necessary for optimal cellular communication (McMahon and Gallop, 2005; Rohrbough and Broadie, 2005). However, despite growing evidence for the critical role of lipids in brain function, little is known about the brain's lipidome composition, the lipid concentration differences among brain regions, and the lipidome differences between the brain and other tissues.

Although the comprehensive identification and quantification of lipid molecules in complex tissues such as the human brain is a daunting task, recent progress in untargeted mass spectrometry (MS)-based lipidome analysis has provided experimental opportunities for the large-scale quantitative profiling of thousands of individual hydrophobic compounds (Harkewicz and Dennis, 2011). To date, this methodology has been used successfully to characterize the membrane lipid composition of *E. coli* (Oursel et al., 2007) as well as the crucial role of lipids in HIV replication (Brügger et al., 2006) and to inspect the lipid changes in brain regions of a mouse model of Parkinson's disease (Rappley et al., 2009). However, it has not yet been applied to the comprehensive characterization of the primate brain lipidome. Given the important role of lipids in the nervous system, knowledge of lipidome features specific to the brain and to its distinct regions, as well as of the evolution of lipidome composition across species, may provide novel insights into the mechanisms and the evolution of brain functionality.

In this study, we used untargeted large-scale MS-based lipidomics to characterize the lipidome composition of three anatomically and functionally distinct brain regions and two non-neural tissues of humans, chimpanzees, macaque monkeys, and mice. We identified differences in lipidome composition among tissues and assessed the evolutionary dynamics of lipidome features across species. Using transcriptome data, measured in the same set of samples using RNA-sequencing (RNA-seq), we identified parallel changes in lipid concentration and expression of the transcripts that encode the corresponding metabolic enzymes. Finally, we identified human-specific lipid composition changes potentially linked to the evolution of cognitive features unique to the human species.

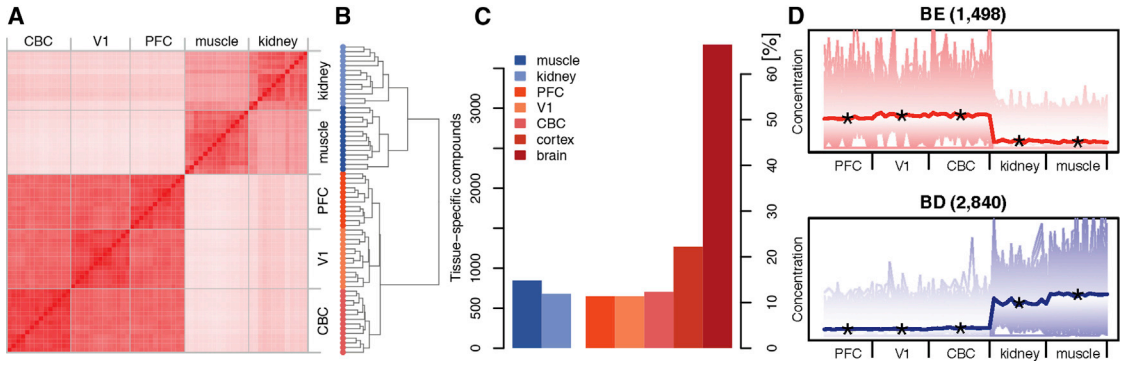

Figure 1. Lipid Concentrations in Brain and Non-Neural Tissues in Humans

(A) Heat map of human tissue samples based on Euclidian distances of lipid concentration levels. Darker shades of red correspond to shorter distances. Samples are ordered according to the dendrogram shown in (B).

(B) Dendrogram of human tissue samples based on Euclidian distances of lipid concentration. The dendrogram was constructed using hierarchical clustering with complete linkage. The node colors indicate the tissue identity of the samples.

(C) Number (left y axis) and percentage (right y axis) of lipids showing concentration levels specific to a given tissue in humans. Numbers of lipids specific to a given brain region were determined by comparison with the most similar brain region in the dataset: PFC to V1 and CBC to cortex.

(D) Clustering of lipids according to their concentrations in human tissues. Shown are lipids in the BE and BD clusters. Samples are ordered along the x axis according to their tissue identity, as indicated below the axis. Shaded areas represent concentration profiles of all individual compounds within a cluster, normalized by their Euclidian norm. Curves represent the average concentration profile of all compounds within a cluster. The star symbols show average normalized concentration levels of all compounds within a cluster in a given tissue. The abbreviated name and the total number of lipid compounds within a cluster are shown above each plot.

RESULTS

Lipidome Measurements

We assessed the repertoire and concentrations of hydrophobic compounds with molecular weights below 3,000 Daltons (henceforth referred to as "lipids" for simplicity) in five tissues: three brain regions (the prefrontal cortex [PFC], primary visual cortex [V1], and cerebellar cortex [CBC]) and two non-neural tissues (the kidney renal cortex and thigh muscle). The two cortical brain regions, PFC and V1, were selected to represent both functionally and transcriptionally distinct regions of the neocortex (Bernard et al., 2012; Hawrylycz et al., 2012; Kang et al., 2011; Lein et al., 2007). To assess the evolutionary dynamics of tissues' lipidome composition and to identify lipidome features unique to humans, we measured lipid concentrations in the same set of tissues in chimpanzees, rhesus macaques, and mice (Supplemental Experimental Procedures available online). In each tissue of each species, lipidome measurements were collected from 14 healthy adult individuals, allowing us to gauge intra-species lipidome variation. In addition to the lipidome measurements, we further analyzed transcriptome data, obtained using RNA-seq, in all five tissues in a subset of six individuals of each species (Bozek et al., 2014).

The lipidome composition of all samples was assessed using liquid chromatography coupled with high-precision mass spectrometry in positive and negative ionization modes (Giavalisco et al., 2011). We quantified a total of 5,713 mass spectrometry features detected in at least seven individuals in one tissue of one species: 4,852 in positive and 861 in negative ionization mode. Among them, 1,991 were annotated using computational matching of the mass spectrometry features to the lipid database entries (Fahy et al., 2009; Figure S1). The annotation procedure was additionally refined by merging MS peaks with matching lipid annotation and highly correlated concentration levels across tissue samples.

To assess the effects of postmortem delay characteristic of human and chimpanzee samples on lipid concentrations, we further analyzed macaque samples collected immediately after death (n = 85) and after a 4- to 6-hr delay (n = 10; Supplemental Experimental Procedures). This analysis revealed significant concentration changes for a total of 516 mass spectrometry features, including 205 annotated compounds ($q < 0.05$ in at least one tissue; Figure S1). These features were excluded from further analysis. Although many human samples had a longer postmortem delay, lipids showing a significant concentration relationship with postmortem delay in humans agreed well with the ones found in macaques (permutations, $p < 0.001$; Supplemental Experimental Procedures). Furthermore, lipids showing a significant concentration relationship with postmortem delay as well as with tissue RNA preservation, age, and sex in any of the four species did not overlap significantly and substantially with lipids showing human-specific lipidome changes (Supplemental Experimental Procedures).

Lipidome Variation across Human Tissues

To examine lipidome differences among human tissues, we inspected the concentration profiles of all 5,713 detected hydrophobic compounds (mass spectrometry features). We observed that, despite substantial individual variation, each tissue and brain region shows distinct lipidome signatures, and the lipid composition of the brain is markedly different from that of the two non-neural tissues (Figures 1A and 1B).

Statistical analysis of lipid concentration differences among the five human tissues confirmed these observations. Of 4,727

compounds showing significant concentration differences between the human brain (PFC, V1, and CBC), kidney, and muscle (t test, $p < 0.01$; permutations, $p < 0.01$), 3,542 (75%) showed concentration profiles specific to the brain; i.e., concentration levels were significantly different in the brain compared with non-neural tissues (t test, $p < 0.01$; permutations, $p < 0.01$; Figure 1C; Figure S2). By contrast, only 13% and 20% of compounds showed concentration profiles specific to kidney and muscle, respectively (Figure 1C). This result was robust to the number of samples used to represent each tissue (Figure S2).

Within the brain, differences in lipid composition among three anatomically and functionally distinct brain regions were less pronounced but still clearly detectable. 445 compounds (8%) showed concentration profiles that differed between the PFC and V1, 562 (10%) were specific to the CBC, and 899 (19%) were specific to the cortex as a whole (t test, $p < 0.01$; permutations, $p < 0.01$) (Figure 1C). Importantly, the separation of the brain from the two non-neural tissues does not occur at the transcriptome level, where all three tissues are approximately equidistant from one another (Figure S2). Therefore, the extensive lipid composition specificity of the brain supports the notion that lipids play special roles in brain functionality.

To investigate the exceptional lipid composition divergence between the brain and the two non-neural tissues, we sorted all 5,713 detected compounds based on their concentration profiles across human tissues. Three main categories emerged: brain-enriched (BE) lipids constituting 26% of all detected compounds, brain-depleted (BD) lipids constituting as many as 50% of all detected compounds, and ubiquitous (UB) lipids present in all tissues at varying concentration levels and constituting the remaining 24% of detected compounds (Figure 1D; Figure S2). Remarkably, each of these categories was enriched in specific and distinct types of lipid molecules (hypergeometric test, $p < 0.01$; permutations, $p < 0.01$) (Table S1). Two discernable lipid concentration patterns were also formed within the brain (Figure S2).

To assess whether lipidome composition differences between the brain and two non-neural tissues could be traced to differences in expression of the corresponding metabolic enzymes, we linked 17,550 genes expressed in the tested tissues to detected lipid compounds, based on the human metabolome database (HMDB) annotation (Wishart et al., 2009), resulting in 1,245 enzymes linked to 1,188 lipid compounds. We found that lipids enriched in brain (BE lipids) show a significantly greater association with metabolic enzymes specifically expressed in the CBC, PFC, V1, and cortex as a whole than would be expected by chance (permutations, $p < 0.05$; Table S2). Therefore, although overall transcriptome differences among tissues do not show a clear brain-specific profile, the expression of metabolic enzymes supports the specific lipidome composition of the brain tissue.

General Features of Lipidome Evolution

We next compared the composition of the human lipidome to that of chimpanzee, macaque, and mouse tissues. Lipid concentration profiles measured in these species generally resembled the lipidome profiles of human tissues. Within each species, the lipidome profiles showed discrete tissue- and brain region-specific concentration signatures, and the lipid composition of the brain differed strikingly from that of non-neural tissues in each species (Figure S3). Furthermore, lipids distinguishing brain from the non-neural tissues (BE and BD lipids) overlapped and correlated significantly among all four species (permutations, $p < 0.01$; Supplemental Experimental Procedures), indicating the general conservation of tissue-specific lipidome features across species.

Despite this general conservation of tissue-specific lipidome features among species, we found a number of important differences. First, although the brain lipidome is clearly distinct from other tissues in all species, the extent of lipid composition divergence between the brain and non-neural tissues varies significantly among species. The largest lipidome divergence between the brain and non-neural tissues was observed in humans, followed by chimpanzees and macaques, with the smallest divergence found in mice (Figure 2A). This was not caused by general differences in lipidome measurements among species because the numbers of detected compounds and compound concentrations did not follow this trend (Figure S3 and Supplemental Experimental Procedures). Therefore, the extent to which the brain lipidome differs from the other two tissues parallels the brain's anatomical and functional complexity among the mammalian species analyzed.

Within the brain, over 73% of 3,556 lipid compounds detected in at least one brain region of one species showed significant concentration differences among the four species (ANOVA, $p < 0.01$; permutations, $p < 0.01$). By assigning these differences to specific evolutionary lineages (t test, $p < 0.01$; permutations, $p < 0.01$), we found that general lipidome divergence largely follows the genetic divergence among the species in the three separate brain regions, cortex, and brain as a whole (Pearson correlation, $r^2 = 0.88$, $p < 0.01$) (Figure 2B) as well as in kidney and skeletal muscle (Pearson correlation, $r^2 = 0.77$, $p < 0.02$). However, the divergent and conserved lipids were not distributed equally among tissue-specific categories. Among primates, lipids enriched in brain (BE lipids) showed an almost 4-fold greater proportion of divergent compounds than BD lipids (Figure 2C). This difference was not caused by the higher concentration of BE lipids in neural tissues; subsampling of BE and BD lipids from the same concentration range did not affect the result (Figure S3). Therefore, concentration levels of lipids enriched in brain evolved at a much more rapid pace than concentration levels of lipids characteristic of non-neural tissues (BD lipids).

Human-Specific Features of Brain Lipidome Evolution

As indicated by the above analysis, we detected two features unique to brain lipidome evolution: greater lipidome divergence between the brain and non-neural tissues in species showing greater cognitive complexity and faster divergence of lipids enriched in brain compared with lipids enriched in non-neural tissues. These features suggest a link between brain lipidome evolution and the evolution of brain functionality—a hypothesis that would be further supported by the existence of lipidome features unique to the human brain lipidome.

To investigate this, we compared lipidome divergence on the human and chimpanzee evolutionary lineages separately in the three brain regions as well as in the cortex and brain as a whole.

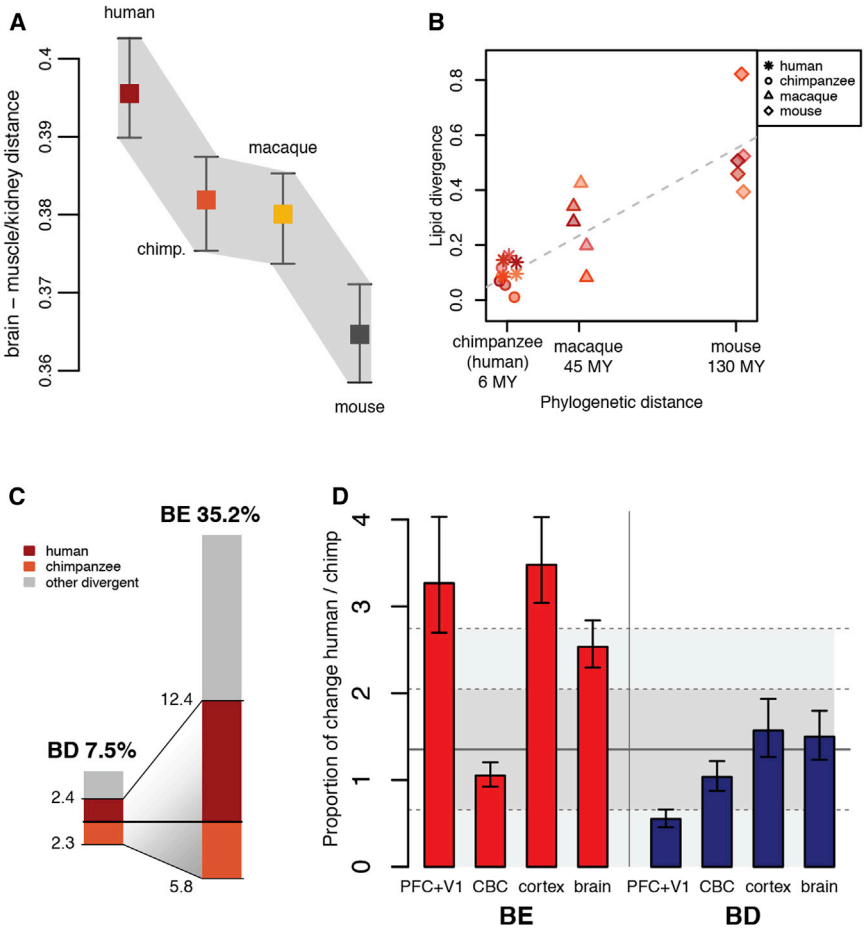

Figure 2. Brain Lipidome Evolution

(A) Average difference between lipid concentration levels in the brain and non-neural tissues in the four species. The squares represent the mean of the concentration level differences. The whiskers extend to the extremes of variation of the mean calculated by random sampling of three-quarters of all detected lipid compounds 1,000 times.

(B) Relationship between species-specific lipid concentration divergence in each brain region, cortex, and brain as a whole and the phylogenetic distance among species. Phylogenetic distance is represented by the time of species divergence from the most recent common ancestor with humans (x axis). Lipid concentration divergence was estimated as the proportion of species-specific lipids in a given tissue among all lipids specific to any species in this tissue (y axis). Each symbol represents this ratio for one tissue in each species. The linear regression between lipid concentration divergence and phylogenetic distance is represented by the dashed line.

(C) Proportions of BD and BE lipids showing significant species-specific concentration differences among primate species in any brain region, cortex, or brain as a whole. The colors and numbers to the left of the bars indicate the percentage of lipids showing human-specific (dark red) and chimpanzee-specific (orange) lipid concentration changes. Changes separating macaques from humans and chimpanzees are represented by the gray parts of the bars. The total percentage of BD and BE lipids showing significant change in any primate species is indicated above the bars.

(D) Ratio of human-specific to chimpanzee-specific lipid concentration changes in different brain regions. The error bars show variation of the ratio estimates calculated by bootstrapping over compounds 1,000 times. The horizontal line represents the average ratio expected by chance calculated by randomizing sample labels 1,000 times. The shaded regions extend to 0.5 and 1 SD of the chance ratio distribution. The brain regions are labeled below the bars. PFC+V1, the ratio based on the sum of species-specific lipids determined in these two brain regions individually; cortex, the ratio based on species-specific lipids determined using two brain regions as a single entity.

In the BD category, approximately equal numbers of lipids showed a concentration divergence on the human (n = 66) and chimpanzee (n = 67) evolutionary lineages. By contrast, BE lipids showed a more than 2-fold excess of concentration changes on the human (n = 186) than on the chimpanzee lineage (n = 87) (Figure 2C). Furthermore, human-specific lipidome changes were not distributed equally among brain regions. The two cortical regions, PFC and V1, showed a more than 3-fold excess of human-specific changes among BE lipids, significantly more than expected by chance (permutations, $p < 0.05$), whereas there was no difference between the amount of human-specific and chimpanzee-specific divergence in the cerebellum (Figure 2D). Notably, BD lipids as well as genes showed no significant differences between human-specific and chimpanzee-specific concentration and expression divergence in any brain region (Figure 2D; Figure S3). These results were robust to the choice of p value cutoff used to define species-specific lipidome changes and to the influence of confounding effects of tissue preservation, postmortem interval length, and individuals' age and sex, as assessed using linear regression tests (Supplemental Experimental Procedures). Therefore, the observed acceleration of lipidome changes on the human evolutionary lineage is particular to BE lipids in the cortex—the region commonly associated with human-specific brain functions—and is not seen in the cerebellum—the region associated with general cognitive tasks such as motor coordination (Ramnani, 2006).

Lipids with Human-Specific Concentrations in the Brain

Lipids showing human-specific concentration changes were enriched in a narrow group of lipid classes (Table S4). Furthermore, three discrete functional units could be distinguished by combining lipid concentration and gene expression changes specific to the human brain (Figure 3A). The identity of lipid compounds in these three units, described below, was confirmed by manual inspection of MS chromatograms.

The first functional unit involves lipids from the diacylglycerophosphocholines (GP0101) lipid subclass of the glycerophosphocholines (GP01) class. Lipids from this group showed predominantly lower concentration levels in the human brain and are linked to two enzymes: phospholipase D family member 6

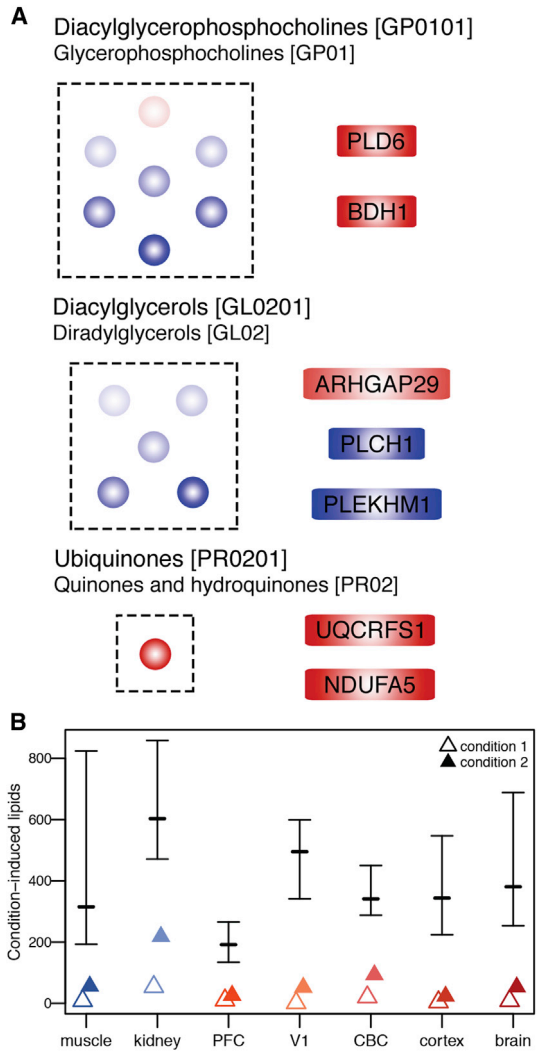

Figure 3. Functional Lipid-Enzyme Units Specific to the Human Brain and Environmental Effects on the Lipidome

(A) Functional units of the BE lipids and their linked enzymes showing human-specific changes in the brain. Each unit is composed of lipid compounds of a specific lipid subclass and their linked enzymes. The coloring of the nodes represents the direction and amplitude of the change of lipid concentration level or enzyme expression level on the human lineage compared with the chimpanzee and macaque lineages. red indicates elevated and blue reduced concentrations on the human lineage. The labels show subclasses (large font) and classes (small font) of the lipids. Enzyme names are indicated in the respective boxes.

(B). Effect of environmental changes on lipid concentration levels. The colored symbols show numbers of lipids with significant lipid concentration differences in every tissue between six macaques subjected to environmental condition 1 (physical activity deprivation) or environmental condition 2 (high nutrition and physical activity deprivation) and all control macaques. Horizontal black bars show average numbers of lipids with significant lipid concentration differences between six humans chosen randomly from all human individuals 1,000 times and all chimpanzees. The error bars extend to the 0.05 and 0.95 quintiles of the average number estimates.

(*PLD6*) and 3-hydroxybutyrate dehydrogenase type 1 (*BDH1*). Both enzymes showed significantly higher expression levels in humans compared with other species and are involved in lipid biosynthesis and binding. The reported functions of these enzymes suggest that this unit may play roles in membrane construction, signaling, and energy metabolism (Choi et al., 2006; Maurer et al., 2011).

The second functional unit involves the diacylglycerols (GL0201) subclass of the diradylglycerols (GL02) lipid class. These lipids also showed decreased concentration levels in the human brain and are linked to three enzymes showing human-specific expression patterns: phospholipase Cη1 (*PLCH1*) and pleckstrin homology domain (*PLEKHM1*), both downregulated in the human brain, and Rho GTPase activating protein 1 (*ARHGAP1*), upregulated in the human brain. The functions of these enzymes are involved in signal transduction, immune response, cancer, and neurological diseases (Tabata et al., 2010; Xu et al., 2013).

The third functional unit involves one lipid compound, coenzyme Q10, representing the ubiquinones (PR0201) subclass of the quinones and hydroquinones (PR02) lipid class, which shows an elevated concentration in the human brain. Although two more ubiquinone compounds, 3-decaprenyl-4,5-dihydroxybenzoic acid and dihydromenaquinone-9 are within the BE cluster and show human-specific concentration levels in the brain, only coenzyme Q10 is linked to enzymes in the database annotation. We show that these enzymes, ubiquinol-cytochrome C reductase, Rieske iron-sulfur polypeptide 1 (*UQCRFS1*), and NADH dehydrogenase (ubiquinone) 1 α subcomplex 5 (*NDUFA5*), also have elevated expression levels in the human brain. These enzymes are involved in oxidative phosphorylation and have been linked with neurodegenerative diseases such as Alzheimer's disease, Huntington's disease, and Parkinson's disease and with autism, suggesting a role for ubiquinone lipids in these neurodegenerative processes (Marui et al., 2011).

Environmental Effects on the Lipidome

Could environmental effects particular to humans explain the excess of human-specific lipidome changes found among BE lipids in certain brain regions? We conducted additional lipidome measurements in adult macaque monkeys that were subjected to altered diet and environmental conditions mimicking some aspects of the modern human lifestyle. Specifically, monkeys were placed for 1 month into indoor solitary standard-size cages with no dietary change (stress and exercise factors, condition 1; n = 6) or with an additional dietary change to a cooked diet with high sugar and fat content (stress, exercise, and diet factors, condition 2; n = 6) (Supplemental Experimental Procedures). Parallel to this treatment, the control macaques, as well as all other macaques used in this study (standard condition, controls; n = 17), were fed a balanced plant-based diet and housed in family groups in spacious outdoor enclosures.

Less than 1% of the 5,713 detected lipids showed significant change under condition 1 and less than 4% under condition 2 in any of the five tissues. For both conditions, the largest effect was observed in the kidney. Each of the environmental perturbations induced substantially fewer lipid concentration changes compared with the lipidome differences observed between the same numbers of randomly sampled chimpanzees and human individuals (Figure 3B). Furthermore, unlike evolutionary changes, lipidome changes induced by environmental effects

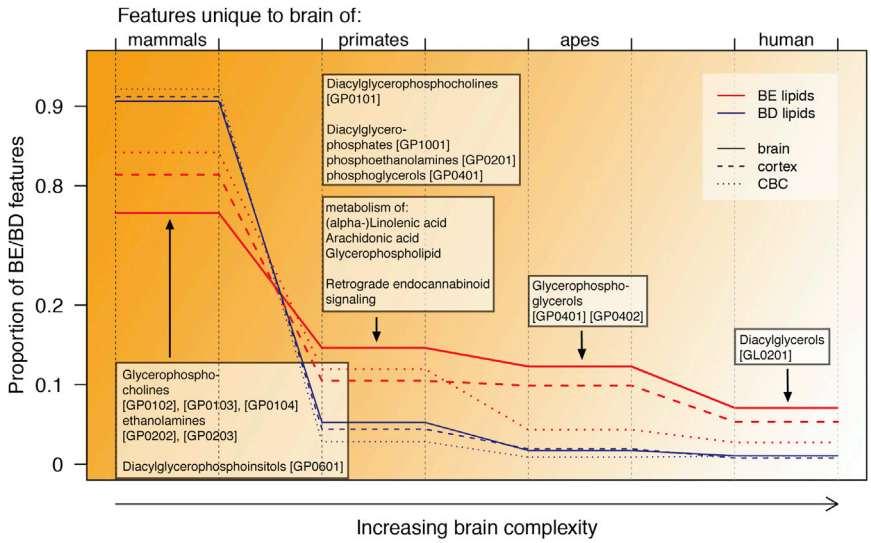

Figure 4. Lipidome Changes in Primate Brain Evolution

The colored lines indicate the proportions of BE and BD lipid compounds in four evolutionary categories: mammals, lipid compounds with concentrations conserved between the three primate species and mouse; primates, lipids conserved among the three primate species and distinct from mouse; apes, lipids conserved between humans and chimpanzees and distinct from macaques; human, lipids with human-specific concentration levels. Lipids were classified in these four categories based on all brain tissue samples (solid line), cortex samples (dashed line), and CBC samples (dotted line). The full list of lipid classes and pathways enriched among lipids in the four evolutionary categories is provided in Table S6.

were not dominated by BE lipids. Instead, lipids in the BD category constituted 57% of the total changes under condition 1 and 54% under condition 2 (Table S5). By contrast, less than 20% of lipids affected by any of the two conditions belonged to the BE lipids. Clearly, our experiment is limited by the spectrum of tested environmental effects and the duration of exposure. Still, similar experiments conducted in mice reproduced some of the gene expression differences observed between human and chimpanzee livers (Somel et al., 2008) and also resulted in a number of evident phenotypic changes (Engelman et al., 1994; Feige et al., 2008; Kohsaka et al., 2007). Moreover, most lipids composing brain tissue are synthesized in the brain and, therefore, are shielded from environmental and dietary changes by the blood-brain barrier (Piomelli et al., 2007; Sherman and Brophy, 2005). This fact, along with the results of our environmental exposure experiment, suggests that environmental and lifestyle differences between humans and other species are unlikely to fully explain the human-specific lipidome changes observed in our study.

DISCUSSION

This study represents the first global characterization of the lipidome of human, chimpanzee, macaque, and mouse tissues, including three functionally and anatomically distinct brain regions. The lipidome analysis, based on 5,713 hydrophobic compounds, combined with a transcriptome analysis of over 17,000 mRNAs, including 1,245 metabolic enzyme transcripts, revealed some of the general characteristics of evolution at both the transcriptome and lipidome levels. We found that, similar to the transcriptome, lipidome composition is generally conserved among species and diverges largely following the genetic distances among species, i.e., following the evolutionary molecular clock.

However, we found several noteworthy features particular to the lipidome. One of these features is the high specificity of the lipid organization of the brain compared with non-neural tissues. 75% of all detected lipids could be assigned exclusively to either neural or non-neural tissues, whereas only 25% of lipids showed such differences between the kidney and skeletal muscle. By contrast, at the transcriptome level, the extent of differences between the brain and non-neural tissues is comparable with that between the kidney and skeletal muscle. The strong separation of lipids between neural and non-neural tissues suggests that they have specialized roles in brain function. Lipids enriched in brain may, therefore, facilitate the unique architectural and dynamic properties of the cellular membranes in brain tissue.

Other features of lipidome evolution lend further support to this notion. The extent of differences in lipidome composition between the brain and non-neural tissues increases in parallel with the increase in brain function capacity from mice to humans. Furthermore, lipids that distinguish brain and non-neural tissues are enriched in specific classes of lipid compounds, suggesting an organizational specificity of the brain lipidome. Concentrations of lipids enriched in brain change four times more rapidly than concentrations of lipids that are depleted in the brain but abundant in non-neural tissues. In addition, we observe a 3-fold acceleration of lipidome evolution in the neocortical regions, but not in the cerebellum, on the human evolutionary lineage compared with the chimpanzee. Again, this human-specific acceleration is specific to lipids enriched in brain and is not observed for lipids depleted in brain but abundant in non-neural tissues or for gene expression changes. Rapid evolution of brain lipids suggests that they may have contributed to the expansion of the neocortex and brain as a whole, as well as the emergence of novel cognitive functions, including those unique to the human neocortex (Figure 4 and Table S6).

Although the lipidome features listed above are not observable at the transcriptome-wide level, correlations between changes in expression of specific metabolic enzymes and the concentration changes of their corresponding lipids can be traced. Gene expression information of the linked metabolic enzymes allows us to validate the quantitative results of lipid concentration measurements and localize lipid compounds within the functional annotation framework.

Taken together, our results demonstrate that the brain lipidome evolves rapidly, suggesting that lipids play important roles in the evolution of brain functionality, including the cognitive capacities unique to the human brain. Although lipidome studies still represent a methodological and analytical challenge, our results demonstrate that an understanding of brain function, its human-specific features, and its dysfunctions is incomplete without knowledge of the lipidome organization of neural tissue.

EXPERIMENTAL PROCEDURES

Lipids were extracted from frozen tissue powder according to Giavalisco et al. (2011). Unsupervised hierarchical clustering using complete linkage was used to distinguish lipid clusters, based on Pearson correlation, as a distance measure. To annotate MS peaks, we used mass searches with a tolerance of 10 ppm against the LIPID MAPS (Fahy et al., 2009) database, followed by correlation analysis to find annotations supported by multiple adducts. To test for enzyme support for lipid clusters or species-specific lipids, first the link between an enzyme and a compound was determined using the HMDB (Wishart et al., 2009).

Human tissues from respective brain banks were obtained according to the brain bank protocols, requiring permission for brain autopsy and use of the tissue for research purpose from the donors or their relatives. The use of human autopsy tissue is considered non-human subject research and is institutional review board-exempt under NIH guidelines. The animal studies were reviewed and approved by the Institutional Animal Care and Use Ethics Committee of the Shanghai Institute for Biological Sciences.

SUPPLEMENTAL INFORMATION

Supplemental Information includes Supplemental Experimental Procedures, three figures, five additional figures, six tables, and 12 additional tables and can be found with this article online at http://dx.doi.org/10.1016/j.neuron.2015.01.003.

ACKNOWLEDGMENTS

This study was supported by the Strategic Priority Research Program of the Chinese Academy of Sciences (Grant XDB13010200), National Natural Science Foundation of China (grants 91331203, 31171232, and 31420103920), National One Thousand Foreign Experts Plan (grants WQ20123100078), Bureau of International Cooperation, Chinese Academy of Sciences (grant GJHZ201313), National Science Foundation (grant BCS-0824531), Russian Science Foundation (grant 14-28-00234), and James S. McDonnell Foundation (grants 22002078 and 220020293). K.B. was supported by a Chinese Academy of Sciences fellowship (2011Y1SB06). We thank Jerome Boyd-Kirkup for help with manuscript preparation.

Received: June 16, 2014
Revised: August 28, 2014
Accepted: December 31, 2014
Published: February 5, 2015

REFERENCES

Bernard, A., Lubbers, L.S., Tanis, K.Q., Luo, R., Podtelezhnikov, A.A., Finney, E.M., McWhorter, M.M., Serikawa, K., Lemon, T., Morgan, R., et al. (2012). Transcriptional architecture of the primate neocortex. Neuron *73*, 1083–1099.

Bozek, K., Wei, Y., Yan, Z., Liu, X., Xiong, J., Sugimoto, M., Tomita, M., Paabo, S., Pieszek, R., Sherwood, C.C., et al. (2014). Exceptional evolutionary divergence of human muscle and brain metabolomes parallels human cognitive and physical uniqueness. PLoS Biol *12*, e1001871.

Brügger, B., Glass, B., Haberkant, P., Leibrecht, I., Wieland, F.T., and Krausslich, H.G. (2006). The HIV lipidome: a raft with an unusual composition. Proc. Natl. Acad. Sci. USA *103*, 2641–2646.

Choi, S.Y., Huang, P., Jenkins, G.M., Chan, D.C., Schiller, J., and Frohman, M.A. (2006). A common lipid links Mfn-mediated mitochondrial fusion and SNARE-regulated exocytosis. Nat. Cell Biol. *8*, 1255–1262.

Engelman, R.W., Day, N.K., and Good, R.A. (1994). Calorie intake during mammary development influences cancer risk: lasting inhibition of C3H/HeOu mammary tumorigenesis by peripubertal calorie restriction. Cancer Res. *54*, 5724–5730.

Fahy, E., Subramaniam, S., Murphy, R.C., Nishijima, M., Raetz, C.R., Shimizu, T., Spener, F., van Meer, G., Wakelam, M.J., and Dennis, E.A. (2009). Update of the LIPID MAPS comprehensive classification system for lipids. J. Lipid Res. *50*, S9–S14.

Feige, J.N., Lagouge, M., Canto, C., Strehle, A., Houten, S.M., Milne, J.C., Lambert, P.D., Mataki, C., Elliott, P.J., and Auwerx, J. (2008). Specific SIRT1 activation mimics low energy levels and protects against diet-induced metabolic disorders by enhancing fat oxidation. Cell Metab *8*, 347–358.

Giavalisco, P., Li, Y., Matthes, A., Eckhardt, A., Hubberten, H.M., Hesse, H., Segu, S., Hummel, J., Kohl, K., and Willmitzer, L. (2011). Elemental formula annotation of polar and lipophilic metabolites using (13) C, (15) N and (34) S isotope labelling, in combination with high-resolution mass spectrometry. Plant J *68*, 364–376.

Harkewicz, R., and Dennis, E.A. (2011). Applications of mass spectrometry to lipids and membranes. Annu. Rev. Biochem. *80*, 301–325.

Hawrylycz, M.J., Lein, E.S., Guillozet-Bongaarts, A.L., Shen, E.H., Ng, L., Miller, J.A., van de Lagemaat, L.N., Smith, K.A., Ebbert, A., Riley, Z.L., et al. (2012). An anatomically comprehensive atlas of the adult human brain transcriptome. Nature *489*, 391–399.

Jacobson, K., Mouritsen, O.G., and Anderson, R.G. (2007). Lipid rafts: at a crossroad between cell biology and physics. Nat. Cell Biol. *9*, 7–14.

Kang, H.J., Kawasawa, Y.I., Cheng, F., Zhu, Y., Xu, X., Li, M., Sousa, A.M., Pletikos, M., Meyer, K.A., Sedmak, G., et al. (2011). Spatio-temporal transcriptome of the human brain. Nature *478*, 483–489.

Kohsaka, A., Laposky, A.D., Ramsey, K.M., Estrada, C., Joshu, C., Kobayashi, Y., Turek, F.W., and Bass, J. (2007). High-fat diet disrupts behavioral and molecular circadian rhythms in mice. Cell Metab. *6*, 414–421.

Lein, E.S., Hawrylycz, M.J., Ao, N., Ayres, M., Bensinger, A., Bernard, A., Boe, A.F., Boguski, M.S., Brockway, K.S., Byrnes, E.J., et al. (2007). Genome-wide atlas of gene expression in the adult mouse brain. Nature *445*, 168–176.

Marui, T., Funatogawa, I., Koishi, S., Yamamoto, K., Matsumoto, H., Hashimoto, O., Jinde, S., Nishida, H., Sugiyama, T., Kasai, K., et al. (2011). The NADH-ubiquinone oxidoreductase 1 alpha subcomplex 5 (NDUFA5) gene variants are associated with autism. Acta Psychiatr Scand *123*, 118–124.

Maurer, G.D., Brucker, D.P., Bahr, O., Harter, P.N., Hattingen, E., Walenta, S., Mueller-Klieser, W., Steinbach, J.P., and Rieger, J. (2011). Differential utilization of ketone bodies by neurons and glioma cell lines: a rationale for ketogenic diet as experimental glioma therapy. BMC Cancer *11*, 315.

McMahon, H.T., and Gallop, J.L. (2005). Membrane curvature and mechanisms of dynamic cell membrane remodelling. Nature *438*, 590–596.

Oursel, D., Loutelier-Bourhis, C., Orange, N., Chevalier, S., Norris, V., and Lange, C.M. (2007). Lipid composition of membranes of Escherichia coli by liquid chromatography/tandem mass spectrometry using negative electrospray ionization. Rapid Commun. Mass Spectrom. *21*, 1721–1728.

Piomelli, D., Astarita, G., and Rapaka, R. (2007). A neuroscientist's guide to lipidomics. Nat. Rev. Neurosci. *8*, 743–754.

Ramnani, N. (2006). The primate cortico-cerebellar system: anatomy and function. Nat. Rev. Neurosci. *7*, 511–522.

Rappley, I., Myers, D.S., Milne, S.B., Ivanova, P.T., Lavoie, M.J., Brown, H.A., and Selkoe, D.J. (2009). Lipidomic profiling in mouse brain reveals differences between ages and genders, with smaller changes associated with alpha-synuclein genotype. J. Neurochem. *111*, 15–25.

Rohrbough, J., and Broadie, K. (2005). Lipid regulation of the synaptic vesicle cycle. Nat. Rev. Neurosci. *6*, 139–150.

Sherman, D.L., and Brophy, P.J. (2005). Mechanisms of axon ensheathment and myelin growth. Nat. Rev. Neurosci. *6*, 683–690.

Somel, M., Creely, H., Franz, H., Mueller, U., Lachmann, M., Khaitovich, P., and Paabo, S. (2008). Human and chimpanzee gene expression differences replicated in mice fed different diets. PLoS One *3*, e1504.

Tabata, K., Matsunaga, K., Sakane, A., Sasaki, T., Noda, T., and Yoshimori, T. (2010). Rubicon and PLEKHM1 negatively regulate the endocytic/autophagic pathway via a novel Rab7-binding domain. Mol Biol Cell *21*, 4162–4172.

Wishart, D.S., Knox, C., Guo, A.C., Eisner, R., Young, N., Gautam, B., Hau, D.D., Psychogios, N., Dong, E., Bouatra, S., et al. (2009). HMDB: a knowledgebase for the human metabolome. Nucleic Acids Res *37*, D603–610.

Xu, J., Zhou, X., Wang, J., Li, Z., Kong, X., Qian, J., Hu, Y., and Fang, J.Y. (2013). RhoGAPs attenuate cell proliferation by direct interaction with p53 tetramerization domain. Cell Rep *3*, 1526–1538.